Journal of The Electrochemical Society, **162** (9) A1683-A1692 (2015)
0013-4651/2015/162(9)/A1683/10/$33.00 © The Electrochemical Society

Effects of Fluoroethylene Carbonate (FEC) on Anode and Cathode Interfaces at Elevated Temperatures

Hosop Shin,[a] Jonghyun Park,[b,z] Ann Marie Sastry,[c] and Wei Lu[a,z]

[a]*Department of Mechanical Engineering, University of Michigan, Ann Arbor, Michigan 48109, USA*
[b]*Department of Mechanical and Aerospace Engineering, Missouri University of Science and Technology, Rolla, Missouri 65401, USA*
[c]*Sakti3, Inc., Ann Arbor, Michigan 48108, USA*

The use of electrolyte additives is one of the most effective and economical ways to improve battery performance by stabilizing the electrode/electrolyte interface. In this work, we identified that fluoroethylene carbonate (FEC), which is one of the important electrolyte additives, had different impacts on anode and cathode, by investigating a graphite anode and a $LiMn_2O_4$ cathode through electrochemical analyses at room and elevated temperatures. In the anode side, the solid electrolyte interphase (SEI) layer derived from FEC exhibited a lower interfacial resistance and excellent thermal stability, showing excellent rate capability and improved cycle retention of cells. In contrast, poor cycling retention and a rapid increase in the interfacial resistance of the cathode were observed at elevated temperature. The poorer performance of the cathode in the FEC-containing cell at elevated temperature was attributed to the formation of a thicker surface layer and to increased Mn dissolution catalyzed by HF, which resulted from FEC dehydrofluorination initiated or accelerated by elevated temperature. Accordingly, it is suggested that the amount of FEC in a full cell must be optimized to minimize the adverse effects of FEC on cathode.

Manuscript submitted April 29, 2015; revised manuscript received May 28, 2015. Published June 9, 2015.

It is well known that lithium-ion (Li-ion) batteries experience significant capacity fade during cycling or storage at elevated temperatures. However, the mechanisms responsible for the capacity fade at elevated temperatures are poorly understood because the capacity fade is caused by several interdependent factors. On anode side, most previous studies have identified the degradation of the solid electrolyte interphase (SEI) layer as the factor primarily responsible for the capacity loss seen at elevated temperatures.[1–4] Temperature-induced reactions, such as SEI decomposition, redox reaction, and electrolyte decomposition, cause changes in the morphology and composition of the SEI layer.[3] Deposition of transition metal ions, which are dissolved from the cathode active materials at elevated temperatures, onto the anode/electrolyte interface also contributes significantly to the degradation of the SEI layer.[5–7] Degradation of the SEI layer results in SEI reformation and growth, during which cyclable lithium ions are additionally consumed due to further electrolyte reduction reactions. Thus, the degraded SEI layer cannot sustain its original properties, which affects the degradation of anode performance.[1,3,7] For instance, an increase in the level of inorganic components present in the SEI layer can lower the ionic conductivity of the SEI layer, which hinders lithium ion transport into/from the anode.[4]

While degradation of the SEI layer has been considered the main contributor to the fade in capacity at the anode side, several factors have been proposed as reasons for the capacity fade that comes from the cathode side. In particular, $LiMn_2O_4$ shows the most severity in terms of (i) the dissolution of cathode materials due to the disproportionation reaction and hydrofluoric acid (HF) attack; (ii) formation of cathode surface films due to continuous decomposition of the electrolyte; (iii) irreversible phase and structure transition (i.e. Jahn-Teller distortion); and (iv) structural instability at higher potential.[4,8–10]

Several modifications have been made to the cathode side in order to improve the poor performance observed at elevated temperatures. For instance, a considerable degree of Mn dissolution, as well as structural instability, have been suppressed by partially substituting Mn with transition metals, such as Co, Cr, or Ni, and coating the surface with diverse metal oxides.[11,12]

Nevertheless, considerable decay in performance was still observed at elevated temperatures in $LiMn_2O_4$/graphite Li-ion cells.[12] Thus, problems associated with the electrode/electrolyte interfaces have attracted considerable attention as key issues that need to be addressed to solve the battery degradation at elevated temperatures. In particular, the instability or poor characteristics of the SEI layer formed on the anode has been identified as a main issue that must be addressed to further enhance battery performance at elevated temperatures.

The use of electrolyte additives has been considered one of the most effective and economical ways to construct a robust and thermally stable SEI layer on the anode side. Electrolyte additives are electrochemically decomposed on the graphite anode before the reductive decomposition of the main organic solvents, and ensure the electrochemical and thermal stability of the SEI layer. The reduction-type additives, such as vinylene carbonate (VC), vinyl ethylene carbonate (VEC), and fluoroethylene carbonate (FEC), have typically been selected to modify the SEI layer on the anode, thereby enhancing battery performance at both room and high temperatures.[13] VC has been widely used to improve the electrochemical performance and thermal stability of Li-ion batteries.[14–22] It has been reported that adding less than 2% VEC to the electrolyte helped improve cell performance due to the modified SEI layer.[23–25]

Many studies have recently been conducted on the effects of FEC on battery performance. It was reported that adding FEC was beneficial to formation of a desirable SEI layer, thereby improving performances of graphite and silicon anodes.[26–32] Despite this recent attention, the fundamental mechanism of FEC decomposition is still controversial in the literature. One potential mechanism suggested that FEC might lose hydrogen fluoride (HF) through dehydrofluorination to form polymers of VC.[13,31] In this case, lithium fluoride (LiF) and poly(vinylene carbonate) were reported as the main species present in the SEI layer on the anode. Another decomposition mechanism involved opening of the five-membered ring, which led to the formation of lithium poly(vinyl carbonate), LiF, and some dimers.[33] A recent ab initio molecular dynamics simulation proposed that both one- and two-electron mechanisms led to the rapid release of F^- to form LiF.[34] Due to these different decomposition mechanisms, there are still discrepancies regarding the nature of the chemical species that constitute the SEI layer formed on the anode side.[29–32] Moreover, a recent study showed conflicting results regarding the influence of FEC on performance of the anode.[35] Therefore, the impact of FEC on the anode still remains unclear.

While previous studies have attempted to elucidate the effects of electrolyte additives on battery performance, emphasizing the properties of the SEI layer on the anode, relatively little attention has been paid to understanding of the effects of electrolyte additives on the cathode side. Recently, Burns et al. claimed that reduced electrolyte oxidation at the cathode side was primarily responsible for the enhanced capacity retention observed at elevated temperatures due to the addition of VC and that the effect of VC at the anode was less

[z]E-mail: parkjonghy@mst.edu; weilu@umich.edu

important.[19] In addition, it was reported that the addition of VC considerably suppressed Fe dissolution from $LiFePO_4$ cathode material at elevated temperatures.[17] However, this was not the case for $LiCoO_2$ cathode material. It was suggested that the VC remaining after formation of the SEI layer reacted with the cathode surface, which led to Co dissolution during high temperature storage.[20] It was also shown that the addition of VEC had significant effects on the surface of the cathode, improving the electrochemical performance of a $LiNo_{0.8}Co_{0.2}O_2$ /Li cell at 50°C.[36] Thus, the use of electrolyte additives clearly affects the cathode side as well as the anode side. An in-depth understanding of the cathode/electrolyte interface driven by electrolyte additives is necessary to fully evaluate the effects of electrolyte additives on the performance of Li-ion batteries. To the best of our knowledge, this is the first effort to systematically study the effects of FEC on the cathode interface at elevated temperatures.

The goal of this work is to improve our understanding of the influence of FEC on both the anode and cathode sides. First, we investigate the effects of FEC on anode (graphite) performance at elevated temperatures. Next, we conduct a comprehensive investigation of the effects of FEC on the performance of the cathode ($LiMn_2O_4$) at elevated temperatures, identifying its mechanisms of action by focusing on Mn dissolution and surface film formation at the surface of the cathode electrode.

Experimental

Electrode preparation and cell fabrication.— Composite electrodes were prepared to investigate effects of FEC on the performance of a graphite anode and a $LiMn_2O_4$ (LMO) cathode. To prepare the graphite electrode, a slurry was prepared by mixing synthetic graphite powder (90 wt%)(Timrex SLP30, Timcal) with a polyvinylidene fluoride (PVdF) binder (10 wt%)(Kureha 7208, Kureha America) dissolved in N-methyl-2-pyrrolidone (NMP) using a SpeedMixer (FlackTek Inc.). The resulting slurry was cast onto a 9 μm-thick copper foil at a constant speed using a 9-mil film applicator with a doctor-blade film coater (MTI corp.). To prepare a LMO slurry, LMO powder (95 wt%)(Electrochemical grade, particle size <5 μm, Sigma-Aldrich), carbon black (5 wt%)(Super C65, Timcal), and PVdF binder (5 wt%) dissolved in NMP solution were mixed. The slurry was cast onto a 15 μm-thick aluminum foil to make the LMO electrode. All composite electrodes were then dried overnight in a vacuum oven at 110°C. The dried electrodes were punched out as disks with an area of 0.785 cm^2 and vacuum-dried again before being used for coin-cell assembly.

To assemble 2032-type coin cells, the working electrode was assembled in a half-cell configuration with a Li foil counter/reference electrode (0.75 mm thick, 99.9%, Alfa Aesar) and a separator (Celgard 2320) soaked in electrolyte solution. The base electrolyte was 1.0 M lithium hexafluorophosphate ($LiPF_6$) dissolved in a 1:1 (by volume) mixture of ethylene carbonate (EC) and dimethyl carbonate (DMC) (Battery grade, <50 ppm HF, <15 ppm H_2O, Sigma Aldrich). FEC (5 wt%) (99% fluoroethylene carbonate, Sigma-Aldrich) was added to the base electrolyte in an aluminum container in order to prepare the FEC-containing electrolyte. The HF content of the FEC-containing electrolyte was less than 50 ppm, as determined by using a non-aqueous titration method. All electrolyte preparation and cell assembly operations were carried out in an argon-filled glove box (M. Braun) at moisture and oxygen levels below 0.1 ppm.

Electrochemical testing: The graphite/electrolyte interface.— The graphite/Li half-cells described above were used for electrochemical experiments, including electrochemical impedance spectroscopy (EIS) measurements, using a battery cycler (Biologic). To evaluate the effects of FEC on the performance of a graphite electrode at room and high temperatures, the half-cells were discharged (lithiation) and charged (de-lithiation) between 5 mV and 1.0 V at constant current (C/18 rate) during the formation process (first 8 cycles). At each cutoff voltage, the voltage was held until the current reached 70 % of the applied current. Subsequent cycles (C/3 rate) before the 31st cycle were performed at room temperature. These cycles were followed by an additional 30 cycles (C/3 rate) at room temperature or 55°C, using a same charge-discharge scheme used in the formation process. All C-rates were based on the theoretical capacity (372 mAh/g) of graphite.

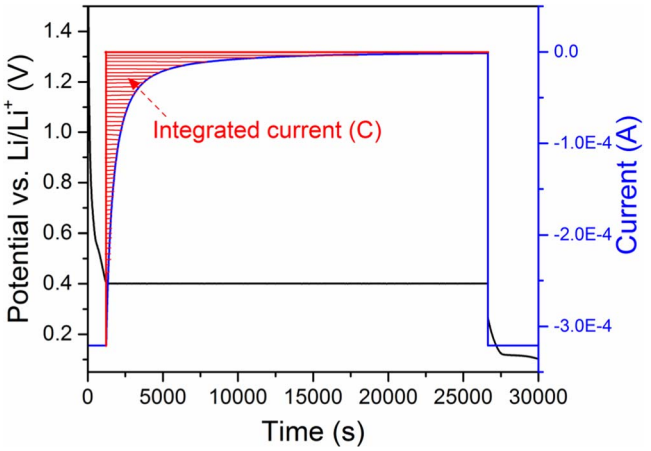

Figure 1. Variations in current (blue) and potential (black) over time during a constant voltage hold at 0.4 V.

To understand the characteristics of the SEI layer formed in the presence of FEC, the interfacial resistances of the cells after the formation cycles and the high temperature cycles (55°C) were measured using EIS. Before the EIS measurements, the potential was held at 1.0 V for 5 h after each cycling. The frequency was scanned from 150 kHz to 50 mHz using a 5 mV amplitude perturbation.

To investigate the stability of the FEC-derived SEI layer at elevated temperature, the change in total reduction charge of the FEC-containing cell, which is the sum of the reversible and irreversible discharge capacities, was compared with that of the FEC-free cell. The cycled cells (8 cycles for formation, followed by 22 cycles at room temperature) were stored at 55°C for 7 days under an open-circuit condition, and then cycling was continued, starting with a reduction current, i.e., discharge of the half-cells.

To further confirm the stability of the FEC-derived SEI layer, the amount of Li-ions consumed during SEI reformation or recovery after high temperature storage was estimated by integrating the currents during constant voltage holds at 0.4 V, which is higher than the potential required for Li-ion intercalation in graphite (below 0.25 V vs. Li/Li^+). For this electrochemical analysis,[37] the cells were cycled at a rate of C/10 between 5 mV and 1.0 V, including the constant voltage holds at each 0.4 V with a cutoff current of <1.5 μA, as shown in Figure 1. With this potential window (1.0 ∼ 0.4 V), it was assumed that a major portion of the Li-ions would be consumed by SEI (re)formation and that the electron flow would be completely balanced by that Li-ion consumption, since Li-ion intercalation was excluded or at least minimized, as described in a previous study.[37] After 15 cycles, the cells were stored at 55°C for 7 days, and then cycling was continued using the same procedure at room temperature.

Electrochemical testing: The LMO/electrolyte interface.— To investigate the effects of FEC on the performance of the LMO cathode at room and high temperatures, the LMO/Li half-cells were cycled between 3.5 V and 4.3 V at a constant current (C/3 rate) during the formation process (first 5 cycles). This was followed by 50 cycles at the same rate, but at different temperatures. For the EIS measurements, the potential was held at 3.5 V for 3 hours and the impedance of the cell was measured by applying a 5 mV amplitude perturbation over the frequency range of 150 kHz to 50 mHz.

Characterizations.— For the surface analysis of the cycled LMO cathode, X-ray photoelectron spectroscopy (XPS) was conducted

using a Kratos Axis Ultra X-ray photoelectron spectrometer equipped with a monochromatic Al Kα excitation source ($h\nu$ = 1486.6 eV). The cycled LMO electrode was rinsed with DMC solvent for 3 min and then vacuum-dried to remove residual salts. Rinsed samples were vacuum-sealed in a glove box and then transferred to the XPS instrument for analysis. The area of the cathode surface layer analyzed was $300 \times 700\ \mu m^2$. The binding energy scale was calibrated based on the graphite peak in the C 1s peak at 284.3 eV. Core spectra were recorded with 20 eV constant pass energy. Charge neutralization was used during the measurements. Depth profiles were obtained by Ar-ion beam sputtering using an ion beam voltage of 4 keV.

To assess the dissolution of manganese from the LMO cathode, the composite LMO electrode was immersed in the electrolyte (1M $LiPF_6$ in EC:DMC) with or without 5 wt% FEC in an aluminum container in a glove box. These aluminum containers were then stored in a vacuum oven for several days. After storage at elevated temperature, the content of Mn dissolved in the electrolyte was determined by inductively coupled plasma optical emission spectrometry (ICP-OES).

To investigate the formation of HF upon thermal aging, the HF content of the electrolyte was measured by an acid-based neutralization titration method.[38] To ensure the accuracy of the measurement, the non-aqueous titration was performed in a glove box, where the content of moisture was maintained below 0.1 ppm. This titration was performed using a 0.01 mol L^{-1} titrating reagent that was prepared by dissolving trimethylamine (Sigma-Aldrich) and a methyl orange indicator (Sigma-Aldrich) in DMC (Sigma-Aldrich). Using this non-aqueous titration method in an inert environment, the HF level of the same electrolyte was determined to be below 50 ppm (∼ 38 ppm), which was in excellent agreement with the reported value (below 50 ppm) by the manufacturer.

Results and Discussion

Anode side: Effects of FEC on the graphite/electrolyte interface.— Figure 2 shows the differential capacity (dQ/dV) curves for the first charging (Li intercalation) of Li/graphite half cells with or without added FEC. A peak, which is associated with the reduction of EC, was observed at 0.6 V (vs. Li/Li^+) in the normal cell without additive, while reduction peaks were observed at higher potentials (1.0 ∼ 0.7 V) in the FEC-containing cell. The reduction peaks at higher potentials are associated with the reduction of FEC, since LUMO energy (0.98 eV) of FEC is lower than that of EC (1.17 eV).[27] This indicates that the reduction of FEC occurred on the anode surface prior to the reduction of EC, which was consistent with other studies.[12,27,28,39] Thus, a FEC-derived SEI layer, which consists of decomposition products of FEC, was formed in the FEC-containing cell, and this modified SEI layer significantly affected the performance of the graphite electrodes.

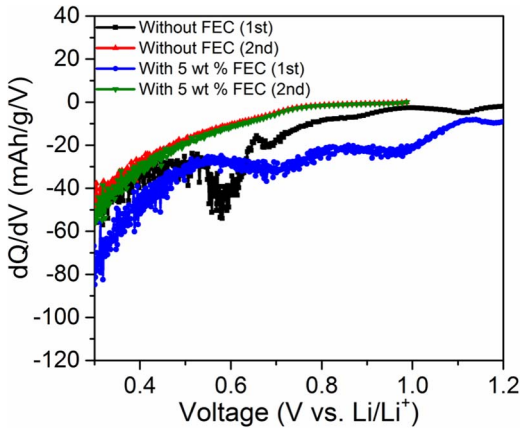

Figure 2. Differential capacity plots of Li/graphite cells with or without added FEC.

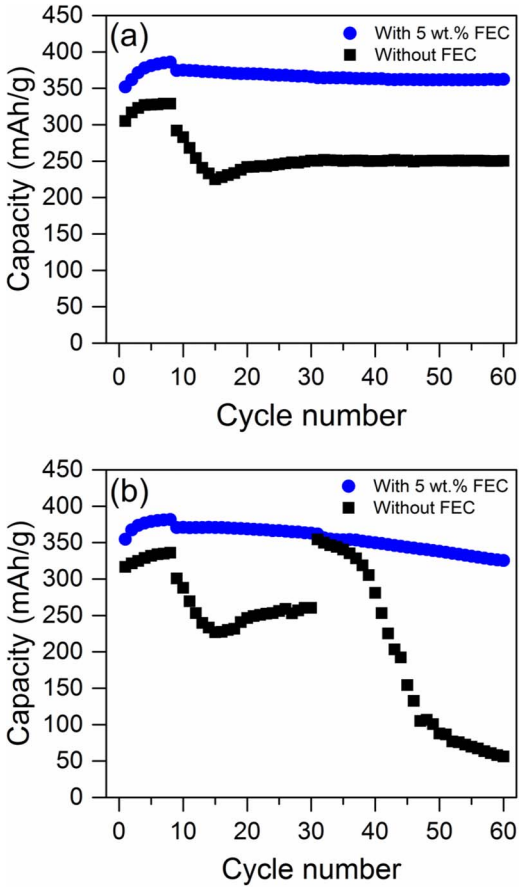

Figure 3. The cycling behavior of Li/graphite cells with or without FEC at (a) room temperature and (b) elevated temperature.

Figure 3 shows the cycling performance of graphite electrodes in FEC-containing and FEC-free solutions at room temperature (Fig. 3a) and at 55°C (Fig. 3b). Graphite/Li cells were cycled at a C/18 rate during the formation phase (first 8 cycles), and then at a C/3 rate during the subsequent cycles at different temperatures.

A gap in the initial specific discharge capacity between the FEC-containing cell and the FEC-free cell was observed. A lower reversible capacity was observed from the FEC-free cell, compared with the FEC-containing cell. It seems that the intercalation/deintercalation of lithium ions into the graphite through an SEI layer derived from a normal electrolyte (1M $LiPF_6$ in EC:DMC) is extremely slow, so that the cell cannot attain the maximum capacity of the graphite electrode, even at a C/18 rate. The faster kinetics of lithium intercalation/deintercalation seen in the presence of FEC can be attributed to a modification of the characteristics of the SEI layer caused by the added FEC.[40,41] As a result, a reversible capacity of 360∼370 mAh/g, which is close to the theoretical maximum capacity of graphite (372 mAh/g), was achieved simply by adding 5 wt% FEC to the electrolyte. This implies that the mobility of lithium ions through the FEC-derived SEI layer was superior to that in the conventional SEI layer, delivering almost the full capacity of graphite at a C/18 rate.

Note that the slight increase in reversible capacity during the formation process (first 8 cycles) was observed regardless of the use of FEC additive. The increased capacity during the initial cycles is consistent with the results of a previous study, in which the same graphite (SLP 30) was used.[42] The increase was due to the slow electrolyte wetting rate in the porous electrode, which consisted of hydrophobic graphite and PvdF.[43,44] Transport of the electrolyte into the pore networks of the electrode is greatly affected by the porosity and thickness of the electrode, as well as the particle morphology of the graphite; a

combination of these factors determines the wetting rate of the electrolyte.

After the formation process, the rate was increased to C/3 during subsequent cycles. In the FEC-free cell, the capacity decreased dramatically and reached its lowest point at 46.4% of the maximum capacity obtained at the C/18 rate. The decreased capacity recovered slightly within a few cycles and the capacity remained at this recovered level through the rest of the cycles. In contrast, the FEC-containing cell showed only a slight drop in capacity when the cycling rate was increased and the cell retained this capacity during cycling. Since the graphite used in FEC-free and FEC-containing cell was the same, the poor capability observed in the FEC-free cell can be attributed to a disruption of the SEI layer formed at the graphite. In other words, the sluggish transport of lithium ions through the SEI layer was primarily responsible for the decrease in capacity at the increased rate, rather than the diffusion length for lithium ions in the graphite particles or the length of the pathways for Li^+ transport to the graphite surface. It can be concluded that the modified SEI layer driven by the addition of FEC exhibited desirable properties for the fast transport of lithium ions and better chemical and mechanical stability at a high rate.

In the FEC-free cell, the observation of a slight recovery of capacity from its lowest point might indicate that the mechanical instability of the conventional SEI layer also contributed to the observed capacity drop at the increased cycling rate. It seems that partial defects in the SEI layer occurred due to the stresses generated during fast (de)intercalation of lithium ions and reformation of the SEI layer, exposing new graphite surfaces.[45] Similar to the previous explanation for the capacity increase during the initial cycles, electrolyte wetting of the new graphite surfaces, as well as restoration of the damaged SEI layer, could result in a slight increase in capacity within a few cycles. It is believed that the local current density and lithium concentration on the particle surface are relatively high for large particles of graphite.[43] The high current density and lithium concentration are likely to cause fast local SEI formation as well as fast local volume changes, with a greater probability of cracks or defects in the SEI layer.[43]

When the temperature increased, most of the reduced reversible capacity was initially recovered in the cell with no additive (Fig. 3b). The increased temperature facilitated the kinetics of lithium ion transfer at the interface, allowing considerable intercalation of lithium ions at the given rate. Additional reduction of the electrolyte at elevated temperatures also might contribute to the initial recovered capacity after the increased temperature. However, the capacity quickly decreased during cycling at the elevated temperature. This is mainly due to the SEI growth at elevated temperatures. SEI growth decreases the conductivity of the graphite agglomerate, and reduces the reversible capacity due to interruption of the lithium ion (de)intercalation.[46] Capacity retention at elevated temperatures improved significantly in the FEC-containing cell, indicating the stability of the FEC-derived SEI layer at elevated temperatures. Therefore, the FEC-derived SEI layer is expected to have desirable properties for the kinetics of lithium ion transfer and excellent stability at high temperature.

The effectiveness of the FEC-derived SEI layer was confirmed by the impedance spectra, as shown in Figure 4. Compared with the FEC-derived SEI layer, the conventional SEI layer formed in the absence of additive showed a higher interfacial resistance, which was displayed as two semicircles in the high and medium frequency ranges, after the formation cycle. Typically, these two suppressed semicircles represent the processes of Li^+ transport through the SEI layer at higher frequencies and the so-called charge-transfer at lower frequencies.[18,28,47] Recent studies have pointed out that the "charge-transfer" process at the graphite/electrolyte interface can be understood as an "ionic transfer" process involving two distinct, but closely interwoven steps: (1) Li^+ desolvation (i.e. stripping of the Li^+ solvation sheath), and (2) the migration of the "naked" Li-ions through the SEI layer.[48,49] Thus, the observed semicircles are correlated with these Li^+ transport processes at the graphite/electrode interface.

As shown in Fig. 4a, the lower interfacial resistance proved that the FEC-derived SEI layer had desirable properties—such as a compact/flexible structure, thin thickness, and better Li^+ conductance—

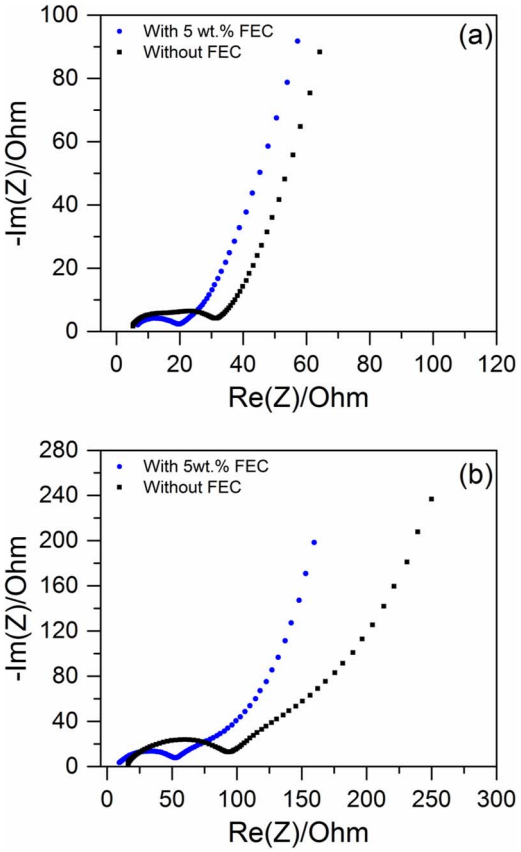

Figure 4. Impedance spectra of Li/graphite cells with or without added FEC after (a) the formation cycle and (b) the 50th cycle at 55°C.

for the faster Li^+ transport at the interface. There has been good agreement that the FEC-derived SEI layer is much thinner and denser than the EC-derived SEI layer.[12,29,32,33] Although there was some discrepancy regarding the composition of the SEI layer derived from the FEC additive,[29,31,33,34] it seems that this SEI layer had better mechanical stability, which allowed it to withstand the stresses that occur during fast intercalation/deintercalation, as well as better passivation, which minimized reactions between anode and electrolyte. As suggested by previous studies, the dense polymeric or oligomeric species that result from FEC decomposition were likely to improve the passivation and flexibility of the SEI layer.[12,32,33]

Figure 4b shows that the stability of the FEC-derived SEI layer was well maintained, even at elevated temperatures. After cycling at high temperature, the increase in the interfacial resistance observed in the FEC-containing cell was significantly lower than that the FEC-free cell. This result implies that the passivation effect of the FEC-derived SEI layer was still effective at elevated temperatures, suppressing further electrolyte decomposition and SEI growth. In contrast, a considerable increase in the interfacial resistance of the normal cell indicates that the conventional SEI layer failed to maintain the passivation and its integrity, possibly due to the dissolution or disruption of the SEI species, leading to continuous electrolyte decomposition and SEI growth. Consequently, a thick and resistive SEI layer could significantly interrupt Li-ion transport at the graphite/electrolyte interface. In addition, the conductivity of the graphite agglomerate would decrease due to poor contact between particles that were covered by the thick SEI layer.

Another noticeable difference was observed at the intercept on the real axis at high frequency, which reflects an ohmic resistance that includes the electrolyte resistance, the electronic resistance between active materials and current collectors, and the external connection resistance.[47] After cycling at high temperature, a higher ohmic

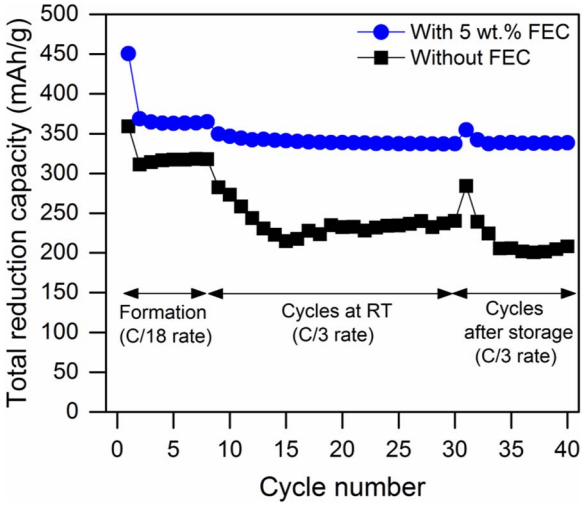

Figure 5. Variations in the total reduction capacity before and after 55°C storage with or without added FEC.

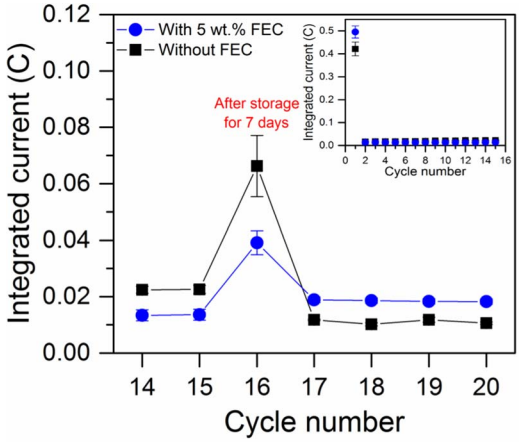

Figure 6. Variations in the integrated current before and after 55°C storage with or without added FEC; the inset figure shows variation of the integrated current during the first 15 cycles.

resistance was observed in the FEC-free cell compared with the FEC-containing cell. This was due to increased electrolyte resistance that may originate from severe electrolyte decomposition and from the chemical species dissolved or decomposed from the SEI layer at elevated temperature. Since the FEC-derived SEI layer was chemically stable at elevated temperature, electrolyte decomposition and SEI dissolution was successfully restrained, allowing no increase in the ohmic resistance.

Next, we further investigated the stability of the SEI layer at elevated temperatures by comparing the results of the total reduction charge over cycling test. As shown in Figure 5, the stability of the FEC-derived SEI layer was compared with that of the conventional SEI layer by examining the total reduction capacity (the sum of the reversible and irreversible discharge capacity) using a method adopted in a previous study.[3] The cells cycled (30 times) at room temperature were stored at 55°C in their deintercalated states, and then cycled again (10 times) at room temperature. The cell with added FEC exhibited a small increase in total reduction charge (17.5 mAh/g) at the 31st cycle, while the cell without additive showed a relatively large increase in total reduction charge (43.9 mAh/g). The additional reduction capacity observed at the 31st cycle was mainly due to the additional reduction of electrolyte, as suggested by the previous study.[3] This result suggests that damage or disruption of the SEI layer formed without additive was severe at elevated temperature, compared with that formed in the presence of added FEC. That is, the FEC-derived SEI layer had better stability against elevated temperature. Note that the total reduction capacity of the cell without additive was lost during continued cycling after storage at high temperature. This indicates that the reconstructed SEI layer did not function effectively as the original SEI layer, which affected the reversibility capacity by disturbing the intercalation and deintercalation of lithium ions.

To further confirm the stability of the FEC-derived SEI layer, we investigated the integrated current, which is indicative of the amount of Li consumed during SEI formation or reformation. Figure 6 displays the consumption of Li ions during the SEI formation process (inset figure), as well as during the SEI reformation process after storage at high temperature. As shown in the inset of Fig. 6, a considerable integrated current occurred during the first cycle, and it decreased significantly after the first cycle. This suggests that the SEI layer was predominantly formed and a major fraction of the Li ions was consumed during the first cycle. This result confirmed that the integrated current could be used as an indicator for estimating the process of SEI formation. The cell with added FEC showed a slightly larger integrated current during the first cycle, compared with the cell with no additive. When we considered the fact that the FEC-derived SEI layer was thinner than the normal layer,[12,32] it might imply that the addition of FEC led to form a denser SEI layer, which might require greater Li-ion consumption. The thermal stability of the FEC-derived SEI layer is demonstrated in the main figure. After storage at high temperature, the FEC-containing cell displayed a slight increase in the integrated current at the 16th cycle, compared with the cell without additive. This result suggests that elevated temperature caused little disruption of the FEC-derived SEI layer, which resulted in a small amount of Li-ion consumption during SEI reformation or SEI recovery. In contrast, the cell without additive consumed a large amount of Li-ions in order to reconstruct the SEI layer that was significantly damaged by elevated temperature.

Cathode side: Effects of FEC on the LMO/electrolyte interface.— Figure 7 shows a comparison of the cycle performance of the LMO electrode in FEC-containing and FEC-free electrolytes at room temperature and 55°C. Unlike the anode (as described in the previous section), at room temperature, there was no distinct difference in capacity retention between the FEC-containing cell and the FEC-free cell, which is quite consistent with a previous report.[12] However, when the cells were cycled at elevated temperature, the FEC-containing cell exhibited worse cycle performance than the FEC-free cell. We believe that the poorer cycle performance at elevated temperature in the FEC-containing cell originated from the LMO/electrolyte side, rather than the Li/electrode side, since it was reported that FEC had a positive

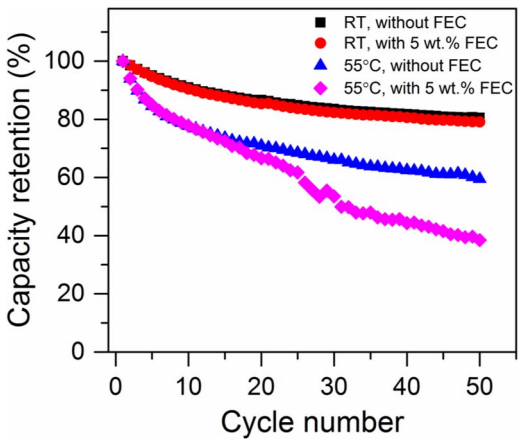

Figure 7. Cycling retentions of Li/LMO cells at room and high temperatures with or without added FEC.

effect on the Li metal electrode, preventing deposition and dissolution of a lithium metal.[50]

The authors of a previous report,[12] concluded that there was little effect of FEC on the LMO cathode side, assuming that the added FEC was quite stable on the positive electrode. It seems that they might have reached a premature conclusion without considering the LMO electrode and its surface at elevated temperature. Here, our results clearly displayed the adverse effect of added FEC on the LMO electrode at elevated temperature. This indicates that the enhanced performance of the FEC-containing LMO/graphite full cell at elevated temperature originates from the superior improvement of the graphite/electrolyte interface, despite of its negative effects, to some extent, on the LMO electrode. Thus, it can be inferred that the FEC remaining after formation of the FEC-derived SEI layer on the anode continuously reacted on the cathode surface, influencing the cathode side, especially at elevated temperature. This suggests that complete consumption of the FEC additive during SEI formation by either controlling the formation procedure or adjusting the content of FEC might be necessary to prevent further reactions at the cathode side.

A previous study regarding the effects of VC lends support to our suggestion.[20] They revealed that VC remaining after formation of the SEI layer on the graphite anode would react continuously on the surface of the cathode, resulting in abrupt evolution of gases, such as CO_2.[20] They also suggested that the dissolution of metal elements on the cathode surface could occur as a result of this reaction. We believe that similar phenomena can occur when FEC is added to the cell. It is important to note that there is a still a chance to further improve the performance of the FEC-containing Li-ion cell at elevated temperature by identifying and solving the problems that occur at the positive electrode. Thus, the rest of this work focused on identifying the reasons behind the poorer cyclability of the LMO electrode in FEC-containing electrolyte, especially at elevated temperature.

Figure 8 shows the impedance spectra of LMO/Li half cells after the 50th cycle in FEC-free and FEC-containing electrolytes at room temperature and 55°C. Consistent with the cycle performance observed above, the impedance of the FEC-containing cell was very similar to that of the FEC-free cell after cycling at room temperature, while there was a clear difference in the cell impedance at high temperature. The difference was primarily observed in the semicircle at the high-to-medium frequency, which represents an interfacial resistance associated with lithium-ion diffusion in the cathode surface layer and the charge transfer process at the cathode/electrolyte interface. Thus, the FEC-containing cell exhibited a rapid increase in the interfacial resistance during cycling at elevated temperature, while a similar interfacial resistance was observed after cycling at room temperature, when compared with the FEC-free cell. The increase in the interfacial resistance (surface film and charge transfer resistances) at elevated temperature might be attributed to poorly conductive

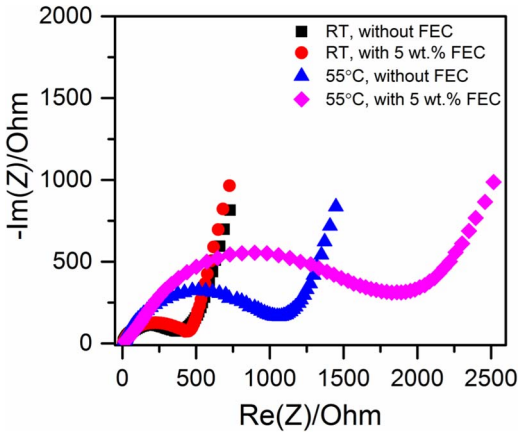

Figure 8. Impedance spectra of Li/LMO cells at room and high temperatures with or without added FEC.

organic and inorganic species resulting from the decomposition of the electrolyte and the inter-particle contact loss induced by manganese dissolution. Since the dissolution of manganese leads to the loss of inter-particle contact as well as the subsequent re-deposition of Mn ions, such as MnO, MnO_2, and MnF_2, the charge transfer resistance is closely coupled with the surface film resistance. The observation of increased interfacial resistance gave us a clue concerning the origin of the poor cycle performance shown by the FEC-containing cell at elevated temperature. It was speculated that added FEC altered the kinetics of surface reactions at elevated temperature. These altered kinetics might accelerate the formation of a surface layer on LMO particles as well as Mn dissolution, lowering both Li-ion transport at the LMO/electrolyte interface and the electronic conductivity of the LMO electrode.

To confirm the above assumption, we first analyzed the thickness and chemical composition of the cathode surface layers that form with/without FEC. The thickness of the surface layer that formed on the cycled LMO electrode in FEC-containing and FEC-free electrolytes was compared based on the depth profile of the LMO electrode (Fig. 9). The relative amounts of the elements (C, F, O, and Mn) changed as a function of sputtering time, since the surface compounds (e.g. surface layer) that covered the LMO electrode were being sputtered away. In particular, the Mn concentration increased as more of the LMO electrode was exposed. After sputtering for a certain time, the Mn concentration became uniform, indicating that the surface layer was fully removed. The dotted line (black) represents a sputter time at which the Mn concentration became uniform. Based on the sputtering time needed for the Mn content to become uniform, the thickness of the cathode surface layer was compared.

As shown in Figs. 9a and 9b, the addition of FEC did not result in a significant change in the thickness of the surface layer that formed after cycling at room temperature. That is, the thickness of the FEC-derived surface layer was very similar to that of the surface layer derived from the normal electrolyte. In contrast, there was a considerable difference in the thickness of the surface layer when the FEC-containing cell was cycled at elevated temperature. After cycling at 55°C, the LMO electrode in the FEC-containing cell was covered with a thicker surface layer (Fig. 9d), compared with the FEC-free cell (Fig. 9c). As mentioned earlier, it seems that FEC-driven surface reactions were more pronounced at elevated temperature, which accelerated the formation of a surface layer on the LMO particles. Thus, the thicker surface layer formed in the FEC-containing cell can hinder fast Li-ion transfer at the interface, contributing to the capacity fade of the cell.

Note that there was no significant difference between the thickness of the surface layer formed after cycling at room temperature (Fig. 9a) and at elevated temperature (Fig. 9c) in the FEC-free cell. This means that the observed decrease in capacity of the FEC-free cell at elevated temperature was mostly caused by increased Mn dissolution at high temperature, rather than by the increased thickness of the cathode surface layer. In the case of the FEC-containing cell, however, the decrease in capacity of the cell at elevated temperature originated not only from increased Mn dissolution but also from the formation of a thicker surface layer on the LMO electrode.

To reveal the mechanisms of surface reactions driven by the addition of FEC, high-resolution XPS spectra were collected from LMO electrodes cycled in FEC-free and FEC-containing electrolytes. As expected, very similar surface layer compositions were observed in FEC-containing and FEC-free cells after cycling at room temperature (Fig. 10a). However, a significant difference in the composition of the surface layer was observed after cycling at high temperature, as shown in Fig. 10b. The FEC-containing cell cycled at high temperature displayed lower intensities of the peaks associated with carbon black (CB, 284.3 eV in C 1s) and lithium manganese oxide (LMO, 529.8 eV in O 1s). This result indicates that the LMO electrode cycled in FEC-containing electrolyte at 55°C was covered by a relatively thick surface layer compared with the FEC-free cell cycled at 55°C. This result is consistent with the result of depth profiling described above. In addition, it was observed that the intensities of other peaks related

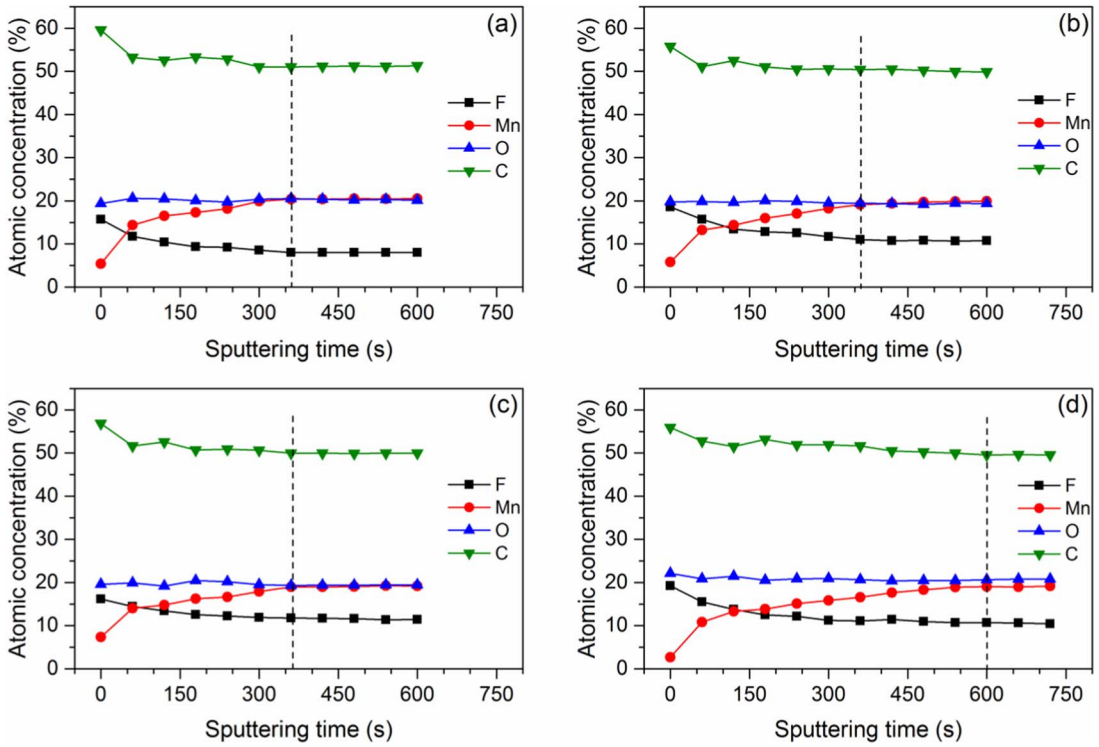

Figure 9. Depth profiles of LMO electrodes after cycling without added FEC at (a) room temperature and (c) 55°C; and with added FEC at (b) room temperature and (d) 55°C. The dotted line (black) represents a sputtering time at which the surface layer is removed and the bulk LMO is fully exposed.

to the surface layer increased considerably in the FEC-containing cell at elevated temperature. It is important to note that the use of FEC yields positive effects on the anode side due to the formation of a thin and dense SEI layer, while it has a negative effect on the cathode side due to the formation of a thick surface layer.

Detailed analysis of the C 1s and O 1s spectra suggested that the main difference between the cells cycled at 55°C in FEC-containing and FEC-free electrolytes was abundance of polymeric species and polycarbonates at the LMO surface. The peak at 285.4 eV in the C 1s spectrum was assigned to polymeric species which might originate from a pure hydrocarbon compound and/or polyethylene oxide (PEO, $(-CH_2-CH_2-O-)_n$).[51,52] The peaks at 286.7 eV and 287.5 –289.5 eV were associated with ether and carbonate functional groups, respectively.[51,52] It is commonly known that these peaks correspond

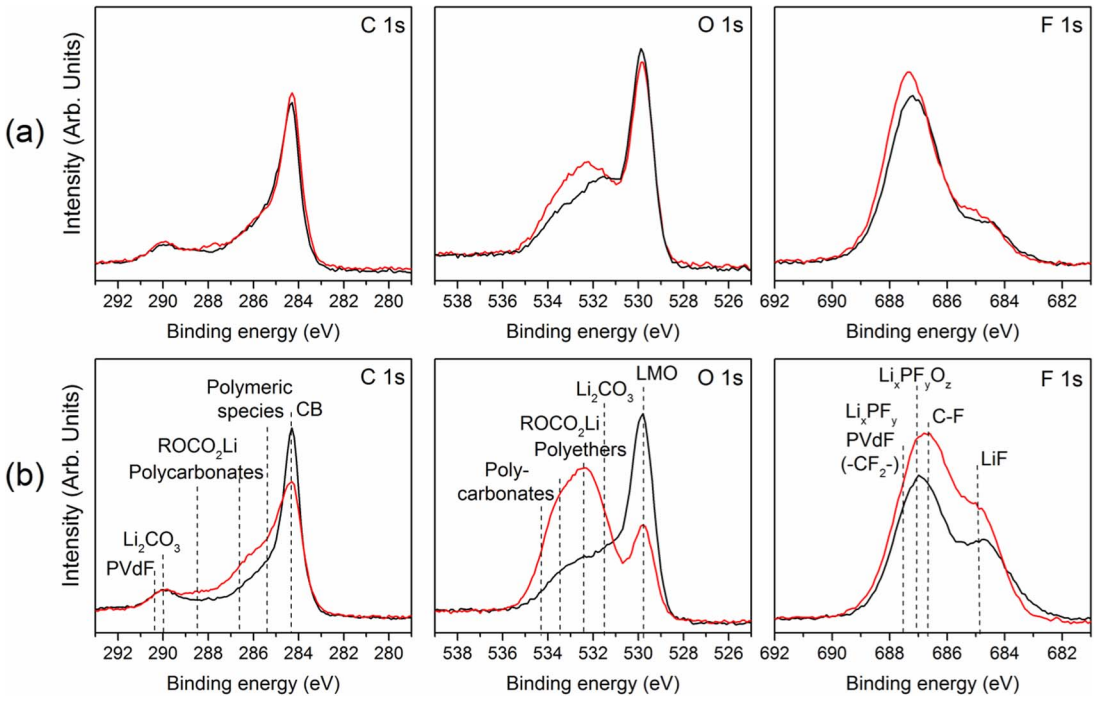

Figure 10. Comparison of XPS spectra of the surface of cycled LMO electrodes with (red) and without (black) added FEC at (a) room temperature and (b) 55°C.

to lithium alkyl carbonates ($ROCO_2Li$) and/or polycarbonates.[10,51,52] Andersson et al. suggested that the carbonate species were probably polycarbonates based on the observation that the transformation of metastable $ROCO_2Li$ into Li_2CO_3 was not seen at elevated temperature in the case of a positive electrode, which was different from the result observed in the case of a negative electrode.[51] Eriksson et al. proposed that the polymerized carbonate formed at elevated temperature resulted from the polymerization of ethylene carbonate (EC), which was initiated by either EC oxidation or the strong Lewis acid PF_5.[52]

We also believe that the increased intensities of the peaks at 286.7 eV and 287.5–289.5 eV were mostly associated with the formation of polycarbonates, since the intensity of the peak (289.9 eV) assigned to Li_2CO_3 did not increase significantly with increasing temperature in our study. Nevertheless, there was still a possibility that the surface layer formed after cycling at room temperature could contain $ROCO_2Li$ species, as suggested in previous studies.[51–53] The abundant presence of PEO-type polymers and polycarbonates in the surface layer derived from the FEC additive at elevated temperature was supported by the dominant intensities of the peaks at 532.5 eV and 533.5∼534.4 eV in the O 1s spectra. The peak at 532.5 eV could be assigned to polyethers (-CH_2O-), which may have originated from oligomers of PEO, while the peak at 533.5∼534.4 eV could correspond to polycarbonates that resulted from EC polymerization and/or polymerization of the FEC additive. Still, the contribution of $ROCO_2Li$ (533.5 eV (C-O-C), 532.5 eV (C=O)) to these peaks, to some extent, cannot be neglected. Thus, it can be inferred that the surface layer formed in the FEC-containing electrolyte contained a significant amount of polycarbonates and polymeric species compared with that formed in the FEC-free electrolyte, especially after cycling at elevated temperature.

The PEO polymer-rich surface layer that formed in the FEC-containing cell might be attributed to additional reactions of $LiPF_6$ with FEC, similar to the reaction of $LiPF_6$ with EC. It has been known that EC polymerization is caused by an acid-catalyzed ring-opening reaction. PF_5, which is a strong Lewis acid, reacts with EC at elevated temperatures, producing PEO polymers and CO_2.[54]

The presence of abundant polycarbonates in the FEC-derived surface layer was likely due to the decomposition and/or side reactions of the FEC additive, initiated or accelerated by elevated temperature. Due to the strong electrostatic field close to the cathode surface, FEC, which is highly polar, is likely to be the preferred target for electrophilic and nucleophilic attack at the cathode.[55,56]

Although the reduction/oxidation or decomposition mechanisms of FEC are not clearly understood, one plausible mechanism is that FEC can be transformed to vinylene carbonate (VC), by the loss of an HF molecule (FEC → VC + HF).[13] In this process, polymerization of the resulting VC could occur, forming polycarbonate species, such as poly(VC). This reaction pathway was previously invoked to explain a high content of polycarbonates in the FEC-derived SEI layer at the anode.[31,32] Similarly, we speculated that vinylene carbonates resulting from FEC decomposition underwent cationic polymerization initiated by protonic and Lewis acids during cycling, producing polycarbonate species on the LMO electrode. Aurbach et al. suggested that oligomers of VC could be produced by cationic polymerization on delithiated oxides (at potentials > 4.2 V vs. Li/Li^+).[14] They reported that an LMO electrode cycled in VC-containing electrolyte exhibited a surface film that mostly contained polycarbonates, possibly poly(VC). Thus, the dehydrofluorination of FEC seems to be the origin of the poly(VC) that forms on the LMO electrode cycled in FEC-containing electrolyte. We believe that the dehydrofluorination of FEC was considerably accelerated by elevated temperature; thus, the majority of the polycarbonates were detected in the surface layer on the LMO electrode cycled in FEC-containing electrolyte at high temperature.

Additional evidence for the accelerated dehydrofluorination of FEC can be found in the F 1s spectra shown in Fig 10b. Assuming that the amounts of LiF generated by the decomposition of $LiPF_6$ ($LiPF_6 \rightarrow LiF + PF_5$) in the FEC-containing cell and the FEC-free cell were similar, the increase in the quantity of LiF seen in the FEC-containing cell was possibly due to the reaction of Li^+ with HF or F^- from the decomposition of FEC at elevated temperature. More interestingly, a peak near 687 eV was observed to have a higher intensity in the FEC-containing cell. It was difficult to precisely interpret the peak, due to the contribution of several compounds (PVdF, Li_xPF_y, and $Li_xPF_yO_z$). Based on the assumption that the decomposition of $LiPF_6$ was not significantly affected by the addition of FEC, the amount of decomposed products, Li_xPF_y and $Li_xPF_yO_z$, were believed to be very similar in both cells. This assumption seemed reasonable because FEC, which has a high dielectric constant, increases the ionization of $LiPF_6$ ($LiPF_6 \leftrightarrow Li^+ + PF_6^-$), thereby suppressing dissociation or decomposition of non-ionized $LiPF_6$ ($LiPF_6 \rightarrow LiF + PF_5$).[57] Therefore, the peak was expected to have a lower intensity in the FEC-containing cell than the FEC-free cell, since the thicker surface layer derived from FEC obscured more of the LMO electrode, including the PVdF binder, as observed in the peaks (CB and LMO) of the C 1s and O 1s spectra. Based on this expectation, it was speculated that additional F-containing compounds were responsible for the increased intensity of the 687 eV peak observed in the spectra of the FEC-containing cell cycled at high temperature. According to recent studies, the additional compounds might be related to dimers containing C-F bonds and/or C-F containing organic products that resulted from FEC decomposition.[33,58]

As mentioned earlier, the decrease in capacity of the FEC-containing cell at elevated temperature could not be solely explained by the formation of a thicker surface layer on the LMO electrode. Mn dissolution from the LMO electrode was another source of battery degradation. According to the mechanism suggested above (FEC → VC + HF), we expected that the FEC-containing electrolyte would produce more HF as a result of FEC dehydrofluorination, or side reactions accelerated by elevated temperature, promoting Mn dissolution. The acid dissolution catalyzed by HF is known to be one of the mechanisms for manganese dissolution at elevated temperature.[43] Thus, any increase in the concentration of HF was likely to lead to considerable dissolution of manganese into the electrolyte.

To further prove the mechanism at elevated temperature, the amount of HF generated as a function of storage time was investigated at elevated temperatures. Figure 11a shows the temperature and time dependence of the quantity of HF in the electrolyte with/without added FEC. Regardless of the use of FEC, the amount of HF in the electrolyte increased with increasing temperature, indicating more $LiPF_6$ decomposition catalyzed by increasing temperature.

The decomposition of $LiPF_6$ typically starts with the following reaction:

$$LiPF_6 \rightarrow LiF + PF_5 \quad [1]$$

which is followed by a reaction between phosphorous pentafluoride and water to form HF and POF_3, as follows:

$$PF_5 + H_2O \rightarrow POF_3 + 2HF \quad [2]$$

Reaction 1 is negligible at room temperature, so $LiPF_6$ is in equilibrium with LiF and PF_5. However, the equilibrium of the reaction is shifted to the right due to the interaction between PF_5 and the solvent at elevated temperatures, lowering the stability of $LiPF_6$.[54,57,59] The reaction rate is dependent on the solvent and the temperature.[54,57] Thus, the increased amount of the strong Lewis acid PF_5 reacts with water, increasing the HF content. Furthermore, the formation of additional HF can be accelerated by the following reactions:[57,59]

$$POF_3 + H_2O \rightarrow POF_2(OH) + HF \quad [3]$$

$$H^+ + PF_6^- \rightarrow HF + PF_5 \quad [4]$$

In addition to the dependence of HF formation on temperature, the time-dependent formation of HF upon thermal aging of the electrolyte was clearly observed. It has been reported that only a small amount of water is needed to start the decomposition reaction and this reaction is accelerated during thermal aging due to various autocatalytic reactions.[59–61] For instance, the released CO_2 from the carbonates during the aging process can be an additional reaction source.[60]

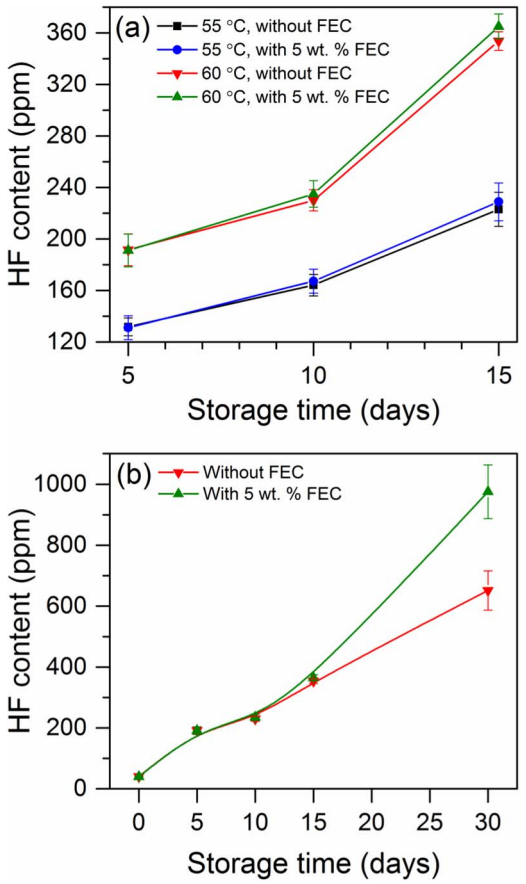

Figure 11. Variation of the amount of HF produced during thermal aging with/without added FEC; (a) 15 days storage at 55°C and 60°C, (b) 30 days storage at 60°C.

More interestingly, the FEC-containing electrolyte produced more HF than the normal electrolyte as storage time increased at elevated temperatures. At room temperature, the amount of HF did not increase until 30 days of storage. There was no significant difference in HF content between the FEC-containing electrolyte and the normal electrolyte.

The difference in the amount of HF produced in the electrolytes during thermal aging became more significant as the temperature and storage time increased. As shown in Fig. 11b, the difference was quite small and unclear until the storage reached 10 days, but it was clearly seen after 10 days. As speculated earlier, it seems that FEC decomposition (such as dehydrofluorination), or side reactions involving FEC, were accelerated by elevated temperature, producing more HF in the FEC-containing electrolyte. Thus, the results suggest that an increased amount of HF can lead to more dissolution of manganese in the LMO cathode. Based on the increase in HF in the FEC-containing cell at elevated temperatures, it also implies that the FEC-derived SEI layer effectively protects the anode from HF attack. It indicates that the FEC-derived SEI layer exhibited the stability against HF attack as well as elevated temperature.

Figure 12 shows the changes in the amount of manganese dissolved from the LMO cathode that was soaked in different electrolytes at elevated temperature as a function of storage time. As expected, we found that the increase in Mn dissolution was accelerated with the use of FEC at elevated temperature. The difference in the amount of dissolved Mn was distinct at the end of 30 days storage. A higher amount of dissolved Mn ions in the FEC-containing electrolyte was associated with the increased HF as a result of FEC dehydrofluorination, which induced acid attack at the LMO cathode by the increased HF. We expected that the effect of increased HF would be more significant

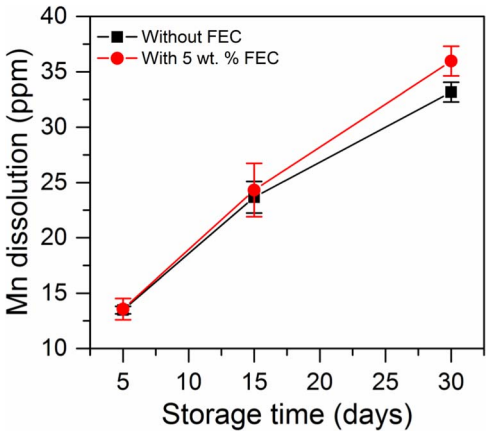

Figure 12. Variation of the amount of dissolved manganese ions with or without added FEC as a function of storage time.

during cycling at elevated temperature, since the disproportionation reaction of Mn^{3+} is promoted by the increased concentration of HF and the thermodynamic instability of delithiated lithium manganese spinel makes it vulnerable to attack by HF; thereby producing more Mn dissolution in the electrolyte.[4,62]

A previous study claimed that the VC-derived SEI layer on the graphite electrode was thermally more stable and could more effectively protect the electrode from the deposition of Mn ions, compared with the FEC-derived SEI layer at elevated temperature.[11] This was based on the assumption that similar amounts of manganese ions were dissolved from the cathode side in the FEC-containing and VC-containing cells. Based on our results, however, it is highly possible that more manganese ions were dissolved from the LMO cathode in the FEC-containing electrolyte than the VC-containing electrolyte. Thereby, the FEC-derived SEI layer was believed to have a difficulty in protecting the graphite/electrolyte interface from Mn deposition due to the considerable amount of dissolved manganese ions released from the cathode side.

Based on our findings, the poor cyclability of the LMO electrode in the FEC-containing electrolyte at elevated temperature was attributed to the increased Mn dissolution and a thicker surface layer as a consequence of acceleration of FEC defhydroluorination in the electrolyte at elevated temperatures.

Conclusions

The effects of the electrolyte additive FEC on electrochemical performance and the electrode/electrolyte interface were thoroughly investigated using graphite/Li cells and LMO/Li cells. The addition of FEC to the normal electrolyte (1M $LiPF_6$ in EC:DMC (1:1 v/v) solution) significantly improved the performance of graphite/Li cells at room temperature and at elevated temperature. This performance improvement was attributed to the stability and effectiveness of the SEI layer resulting from the FEC additive. The FEC-derived SEI layer imparted desirable properties to graphite/Li cells at room temperature, including higher reversibility and excellent rate capability. The lower interfacial resistance observed after the formation cycles of the FEC-containing cell, compared with that of the FEC-free cell, demonstrated that the FEC-derived SEI layer was effective in facilitating Li-ion transfer at the graphite/electrolyte interface. The superior thermal stability of the FEC-derived SEI layer was also confirmed, showing excellent performance during cycling and storage at elevated temperature.

On the other hand, the adverse effect of FEC on the performance of LMO/Li cells was observed at elevated temperature, while there was no clear difference in the performance of LMO/Li cells at room temperature. For the FEC-containing cell, formation of a thick surface layer on the LMO cathode and increased Mn dissolution catalyzed

by elevated HF levels were responsible for the poor performance observed, resulting in a dramatic increase in the interfacial resistance as well as accelerated capacity fading at elevated temperature. It was proposed that the origin of the thick surface layer and the increased Mn dissolution was the FEC dehydrofluorination reaction and/or its side reactions at the LMO surface, initiated or accelerated by elevated temperature. This suggestion was supported by the observation of abundant polycarbonates, possibly poly(VC), on the LMO surface and an increased HF content in the FEC-containing cell at elevated temperature.

Based on our findings, it is suggested that the FEC remaining after formation of the SEI layer on the anode side is detrimental to the cathode side, especially at elevated temperature. It is, therefore, important to optimize the amount of FEC added to the electrolyte in order to minimize the adverse effect of residual FEC on the cathode side. This strategy can be an effective way to further improve the performance of LMO/graphite cells at elevated temperature.

Acknowledgments

The authors acknowledge support provided by the Assistant Secretary for Energy Efficiency and Renewable Energy, Office of Vehicle Technologies of the U.S. Department of Energy under Contract No. DE-AC02-05CH11231, under the Batteries for Advanced Transportation Technologies (BATT) Program subcontract #6906363, with additional sponsorship by the General Motors/University of Michigan Advanced Battery Coalition for Drivetrains.

References

1. A. M. Andersson, K. Edstrom, N. Rao, and A. Wendsjo, *J. Power Sources*, **81**, 286 (1999).
2. T. Zheng, A. S. Gozdz, and G. G. Amatucci, *J. Electrochem. Soc.*, **146**, 4014 (1999).
3. A. M. Andersson and K. Edstrom, *J. Electrochem. Soc.*, **148**, A1100 (2001).
4. J. Vetter, P. Novak, M. R. Wagner, C. Veit, K. C. Moller, J. O. Besenhard, M. Winter, M. Wohlfahrt-Mehrens, C. Vogler, and A. Hammouche, *J. Power Sources*, **147**, 269 (2005).
5. S. Komaba, N. Kumagai, and Y. Kataoka, *Electrochim. Acta*, **47**, 1229 (2002).
6. H. Shin, J. Park, A. M. Sastry, and W. Lu, *J. Power Sources*, **284**, 416 (2015).
7. C. Delacourt, A. Kwong, X. Liu, R. Qiao, W. L. Yang, P. Lu, S. J. Harris, and V. Srinivasan, *J. Electrochem. Soc.*, **160**, A1099 (2013).
8. M. Mohamedi, D. Takahashi, T. Itoh, and I. Uchida, *Electrochim. Acta*, **47**, 3483 (2002).
9. T. Doi, M. Inaba, H. Tsuchiya, S. K. Jeong, Y. Iriyama, T. Abe, and Z. Ogumi, *J. Power Sources*, **180**, 539 (2008).
10. H. Duncan, D. Duguay, Y. Abu-Lebdeh, and I. J. Davidson, *J. Electrochem. Soc.*, **158**, A537 (2011).
11. I. H. Cho, S. S. Kim, S. C. Shin, and N. S. Choi, *Electrochem. Solid St.*, **13**, A168 (2010).
12. M. H. Ryou, G. B. Han, Y. M. Lee, J. N. Lee, D. J. Lee, Y. O. Yoon, and J. K. Park, *Electrochim. Acta*, **55**, 2073 (2010).
13. S. S. Zhang, *J. Power Sources*, **162**, 1379 (2006).
14. D. Aurbach, K. Gamolsky, B. Markovsky, Y. Gofer, M. Schmidt, and U. Heider, *Electrochim. Acta*, **47**, 1423 (2002).
15. D. Aurbach, J. S. Gnanaraj, W. Geissler, and M. Schmidt, *J. Electrochem. Soc.*, **151**, A23 (2004).
16. H. Ota, Y. Sakata, A. Inoue, and S. Yamaguchi, *J. Electrochem. Soc.*, **151**, A1659 (2004).
17. H. C. Wu, C. Y. Su, D. T. Shieh, M. H. Yang, and N. L. Wu, *Electrochem. Solid St.*, **9**, A537 (2006).
18. L. Chen, K. Wang, X. Xie, and J. Xie, *J. Power Sources*, **174**, 538 (2007).
19. J. C. Burns, G. Jain, A. J. Smith, K. W. Eberman, E. Scott, J. P. Gardner, and J. R. Dahn, *J. Electrochem. Soc.*, **158**, A255 (2011).
20. J. Y. Eom, I. H. Jung, and J. H. Lee, *J. Power Sources*, **196**, 9810 (2011).
21. N. N. Sinha, A. J. Smith, J. C. Burns, G. Jain, K. W. Eberman, E. Scott, J. P. Gardner, and J. R. Dahn, *J. Electrochem. Soc.*, **158**, A1194 (2011).
22. B. Li, Y. Wang, H. Rong, Y. Wang, J. Liu, L. Xing, M. Xu, and W. Li, *J. Mater. Chem. A*, **1**, 12954 (2013).
23. Y. S. Hu, W. H. Kong, L. Hong, X. J. Huang, and L. Q. Chen, *Electrochem. Commun.*, **6**, 126 (2004).
24. Y. S. Hu, W. H. Kong, Z. X. Wang, H. Li, X. J. Huang, and L. Q. Chen, *Electrochem. Solid St.*, **7**, A442 (2004).
25. H. Xiang, J. Chen, and H. Wang, *Ionics*, **17**, 415 (2011).
26. R. McMillan, H. Slegr, Z. X. Shu, and W. D. Wang, *J. Power Sources*, **81**, 20 (1999).
27. N. S. Choi, K. H. Yew, K. Y. Lee, M. Sung, H. Kim, and S. S. Kim, *J. Power Sources*, **161**, 1254 (2006).
28. I. A. Profatilova, S. S. Kim, and N. S. Choi, *Electrochim. Acta*, **54**, 4445 (2009).
29. H. Nakai, T. Kubota, A. Kita, and A. Kawashima, *J. Electrochem. Soc.*, **158**, A798 (2011).
30. S. Dalavi, P. Guduru, and B. L. Lucht, *J. Electrochem. Soc.*, **159**, A642 (2012).
31. V. Etacheri, O. Haik, Y. Goffer, G. A. Roberts, I. C. Stefan, R. Fasching, and D. Aurbach, *Langmuir*, **28**, 965 (2012).
32. A. Bordes, K. Eom, and T. F. Fuller, *J. Power Sources*, **257**, 163 (2014).
33. X. Chen, X. Li, D. Mei, J. Feng, M. Y. Hu, J. Hu, M. Engelhard, J. Zheng, W. Xu, J. Xiao, J. Liu, and J. G. Zhang, *Chemsuschem*, **7**, 549 (2014).
34. K. Leung, S. B. Rempe, M. E. Foster, Y. Ma, J. M. M. del la Hoz, N. Sai, and P. B. Balbuena, *J. Electrochem. Soc.*, **161**, A213 (2014).
35. N. N. Sinha, J. C. Burns, and J. R. Dahn, *J. Electrochem. Soc.*, **160**, A709 (2013).
36. J. Li, W. Yao, Y. S. Meng, and Y. Yang, *J. Phys. Chem. C*, **112**, 12550 (2008).
37. A. Mukhopadhyay, A. Tokranov, X. Xiao, and B. W. Sheldon, *Electrochim. Acta*, **66**, 28 (2012).
38. S. H. Youn, Method for measuring HF content in lithium secondary battery electrolyte and analytical reagent composition used in the same, in *U. S. Pat.* (2013).
39. M. J. Chun, H. Park, S. Park, and N. S. Choi, *RSC Adv.*, **3**, 21320 (2013).
40. K. Abe, H. Yoshitake, T. Kitakura, T. Hattori, H. Y. Wang, and M. Yoshio, *Electrochim. Acta*, **49**, 4613 (2004).
41. J. Vetter, H. Buqa, M. Holzapfel, and P. Novak, *J. Power Sources*, **146**, 355 (2005).
42. S. F. Lux, T. Placke, C. Engelhardt, S. Nowak, P. Bieker, K. E. Wirth, S. Passerini, M. Winter, and H. W. Meyer, *J. Electrochem. Soc.*, **159**, A1849 (2012).
43. H. Buqa, D. Goers, M. Holzapfel, M. E. Spahr, and P. Novak, *J. Electrochem. Soc.*, **152**, A474 (2005).
44. W. Pfleging and J. Proella, *J. Mater. Chem. A*, **2**, 14918 (2014).
45. L. Mickelson, H. Castro, E. Switzer, and C. Friesen, *J. Electrochem. Soc.*, **161**, A2121 (2014).
46. C. S. Wang, A. J. Appleby, and F. E. Little, *J. Electroanal. Chem.*, **497**, 33 (2001).
47. Y. Zhang and C. Y. Wang, *J. Electrochem. Soc.*, **156**, A527 (2009).
48. K. Xu, *J. Electrochem. Soc.*, **154**, A162 (2007).
49. K. Xu, A. von Cresce, and U. Lee, *Langmuir*, **26**, 11538 (2010).
50. R. Mogi, M. Inaba, S. K. Jeong, Y. Iriyama, T. Abe, and Z. Ogumi, *J. Electrochem. Soc.*, **149**, A1578 (2002).
51. A. M. Andersson, D. P. Abraham, R. Haasch, S. MacLaren, J. Liu, and K. Amine, *J. Electrochem. Soc.*, **149**, A1358 (2002).
52. T. Eriksson, A. M. Andersson, C. Gejke, T. Gustafsson, and J. O. Thomas, *Langmuir*, **18**, 3609 (2002).
53. T. Eriksson, A. M. Andersson, A. G. Bishop, C. Gejke, T. Gustafsson, and J. O. Thomas, *J. Electrochem. Soc.*, **149**, A69 (2002).
54. S. E. Sloop, J. B. Kerr, and K. Kinoshita, *J. Power Sources*, **119**, 330 (2003).
55. D. Aurbach, Y. Talyosef, B. Markovsky, E. Markevich, E. Zinigrad, L. Asraf, J. S. Gnanaraj, and H. J. Kim, *Electrochim. Acta*, **50**, 247 (2004).
56. T. R. Jow, K. Xu, O. Borodin, and M. Ue, *Electrolytes for lithium and lithium-ion batteries*, p. 93, Springer-Verlag New York (2014).
57. T. Kawamura, S. Okada, and J. Yamaki, *J. Power Sources*, **156**, 547 (2006).
58. E. Markevich, G. Salitra, K. Fridman, R. Sharabi, G. Gershinsky, A. Garsuch, G. Semrau, M. A. Schmidt, and D. Aurbach, *Langmuir*, **30**, 7414 (2014).
59. S. F. Lux, J. Chevalier, I. T. Lucas, and R. Kostecki, *ECS Electrochem. Lett.*, **2**, A121 (2013).
60. L. Terborg, S. Weber, F. Blaske, S. Passerini, M. Winter, U. Karst, and S. Nowak, *J. Power Sources*, **242**, 832 (2013).
61. A. V. Plakhotnyk, L. Ernst, and R. Schmutzler, *J. Fluorine Chem.*, **126**, 27 (2005).
62. J. Wang, Q. Zhang, X. Li, Z. Wang, H. Guo, D. Xu, and K. Zhang, *Phys. Chem. Chem. Phys.*, **16**, 16021 (2014).